AGU PUBLICATIONS

Geophysical Research Letters

RESEARCH LETTER
10.1002/2018GL077253

Key Points:
- The June 2017 heatwave that affected western and central Europe was the earliest European mega-heatwave of the reanalysis period
- The event was associated with a record-breaking subtropical ridge. Dynamical and thermodynamical trends contributed to its exceptionality
- This episode could be a good example of future mega-heatwaves occurring earlier in the summer

Supporting Information:
- Supporting Information S1

Correspondence to:
A. Sánchez-Benítez,
antsan08@ucm.es

Citation:
Sánchez-Benítez, A., García-Herrera, R., Barriopedro, D., Sousa, P. M., & Trigo, R. M. (2018). June 2017: The earliest European summer mega-heatwave of reanalysis period. *Geophysical Research Letters*, *45*, 1955–1962. https://doi.org/10.1002/2018GL077253

Received 12 DEC 2017
Accepted 30 JAN 2018
Accepted article online 5 FEB 2018
Published online 19 FEB 2018

June 2017: The Earliest European Summer Mega-heatwave of Reanalysis Period

A. Sánchez-Benítez[1,2], R. García-Herrera[1,2], D. Barriopedro[2], P. M. Sousa[3], and R. M. Trigo[3]

[1]Departamento de Física de la Tierra y Astrofísica, Facultad de Ciencias Físicas, Universidad Complutense de Madrid, Madrid, Spain, [2]Instituto de Geociencias, CSIC-UCM, Madrid, Spain, [3]Instituto Dom Luiz, Facultade de Ciências, Universidade de Lisboa, Lisbon, Portugal

Abstract This paper examines the characteristics of the heatwave that affected western and central Europe in June 2017. Using a novel algorithm, we show that its extension, intensity, and persistence were comparable to those of other European mega-heatwaves, but it occurred earlier in the summer. The most affected area was Iberia, which experienced devastating forest fires with human casualties and the warmest temperatures of the reanalysis period from daily to seasonal scales. The peak of the mega-heatwave displayed an unprecedented warm air intrusion due to a record-breaking subtropical ridge with signatures closer to those of July and August. The atmospheric circulation was the main triggering factor of the event. However, thermodynamical changes of the last decades made a substantial contribution to the event, by increasing the likelihood of surpassing high-temperature thresholds. This episode could be a good example of a coming future, with high-summer mega-heatwaves occurring earlier.

1. Introduction

Europe has recently experienced summer mega-heatwaves (Bador et al., 2017; Barriopedro et al., 2011; Fischer, 2014; García-Herrera et al., 2010), which stand out from typical heatwaves due to their large spatial extension, intensity, and persistence. The most documented events are the August 2003 event over western and central Europe (e.g., Bador et al., 2017; Fischer, 2014; García-Herrera et al., 2010; Trigo et al., 2005) and the July–August 2010 event in eastern Europe and Russia (e.g., Barriopedro et al., 2011; Dole et al., 2011; Fischer, 2014). Based on the characteristics of these events, Barriopedro et al. (2011) defined mega-heatwaves as regional mean (≥1,000,000 km^2) temperature anomalies of extraordinary amplitude (≥3 standard deviations) at subseasonal scales (≥7 days). However, there is not a universally accepted definition of mega-heatwave and other recent events have been reported in the literature. For example, using the Heat-Wave Magnitude Intensity daily (HWMId), Russo et al. (2015) described the top 11 events since 1950. They are associated, among others, with extensive crop failures (Lesk et al., 2016) and devastating wildfires (Gouveia et al., 2016; Hodzic et al., 2007). These events are also important for human health and wellbeing since, combined with poor air quality (Konovalov et al., 2011; Vautard et al., 2005), they can lead to increased mortality (Haines et al., 2006; Kovats & Hajat, 2008), especially in the elderly people (Fouillet et al., 2006). In particular, the 2003 event caused 70,000 heat-related fatalities and US$10 billions of economic losses (García-Herrera et al., 2010), with similar figures (50,000 fatalities and US$15 billions) for the 2010 event (Barriopedro et al., 2011).

Using the analogue method (Yiou et al., 2014), Jézéquel et al. (2017) found that in most cases the dynamics was the main contributing factor to the temperature anomaly recorded during recent mega-heatwaves, with the only exception of August 2003. Moreover, previous studies have recognized the additional contribution of land-atmosphere coupling during dry periods (Fischer et al., 2007; Miralles et al., 2014; Seneviratne et al., 2010) or sea surface temperature (SST) anomalies (Della-Marta et al., 2007; Duchez et al., 2016). The atmospheric circulation during heatwaves is typically characterized by anomalously high pressure systems, which enhance solar radiative heating, warm advection from lower latitudes, and subsidence (Sousa et al., 2017). Mega-heatwaves have often been related with atmospheric blocking (Dole et al., 2011; Trigo et al., 2005), which are high-latitude persistent slow-moving high pressure systems that interrupt the westerly jet stream (Barriopedro et al., 2006; Pfahl, 2014). However, García-Herrera et al. (2010) and Sousa et al. (2017) concluded that there have been some overstatements when attributing mega-heatwaves to standard high-latitude atmospheric blocking. In fact, extremely warm conditions in southern Europe rather occur under subtropical

ridges extending from subtropical to midlatitudes, which are comparatively narrower and more transient than blocking.

Under the ongoing climate change, mega-heatwaves are becoming more frequent, intense, and longer (Meehl & Tebaldi, 2004; Russo et al., 2015; Schoetter et al., 2015), and this trend is expected to continue in the future. In addition, the earlier onset of the summer season in Europe found in observations (~4 days decade^{-1} from 1979 to 2012; Peña-Ortíz et al., 2015), which is expected to sustain in future projections (Cassou & Cattiaux, 2016), could extend the occurrence of mega-heatwaves to unusual dates when compared to the historical record.

In this context, June 2017 was marked by extremely high temperatures across western Europe. It was the hottest June in Spain (since 1965; AEMET, 2017), where some local records were exceeded by more than 1 °C, and in the Netherlands (since 1901; KNMI, 2017). This month was also the second warmest June in France (since 1900; Meteofrance, 2017) and in Switzerland (since 1864; Meteosuisse, 2017). At daily time-scales, record-breaking maximum temperatures were seen in many Iberian observatories, locally surpassing 45 °C, mainly between 15 and 18 June. Extreme conditions were also reported in other countries across western and central Europe, reaching the UK (34.5° at Heathrow airport in 21 June, the warmest June day since 1976), and not only for day-time temperatures: France set a new national average daily mean temperature record for June of 26.4 °C and Switzerland experienced the warmest June night since 1981, with minimum temperatures above 25 °C in many places.

In spite of this, a noticeably increase in mortality was not reported by the media, arguably due to (i) an efficient implementation of early warning systems following the lessons learned from previous high-impact European mega-heatwaves, such as that of August 2003 (Kirch et al., 2005; García-Herrera et al., 2010; Lowe et al., 2011), and (ii) the use of air conditioning systems (Carmona et al., 2017; Kalvelage et al., 2014), which caused a 15% increase in energy demand in Iberia during the heatwave period (Red Eléctrica Española, http://www.ree.es/es), reaching the highest value of the June time series (starting in 2010). The extreme temperatures were accompanied by drought conditions across western Europe (García-Herrera et al., 2018) and record-breaking SSTs in the eastern Atlantic and the Mediterranean (Climate Central, 2017). The Portuguese wildfires were probably the most dramatic impact of this event, with several large fires deflagrating in central Portugal between 16 and 23 June being responsible for roughly 30,000 hectares of burned area. However, it was the human impact of these fires that was particularly striking, with 64 fatalities registered in just a few hours on 17 June, simultaneously with the destruction of more than 200 houses, numerous cars, and most communication networks in the area.

This paper analyses the life cycle of this event and its relevance at different time-scales through a novel detection scheme. The associated synoptic patterns and their dynamical contribution to the extreme temperatures are then examined, showing the dominant role of an advanced record-breaking subtropical ridge. We also find that the recent climate evolution has made this event more extreme.

2. Data and Methods

Daily mean fields, including temperature at 2 m (T2m) and 850 hPa (T850), and geopotential height at 500 hPa (Z500) were extracted from the National Centers for Environmental Prediction/National Center for Atmospheric Research reanalysis (Kalnay et al., 1996) with a 2.5° × 2.5° resolution for the 1948–2017 period. Daily anomalies were computed removing the 1981–2010 mean for each calendar day. We obtained similar results for other reanalysis products (e.g., ERA-Interim; Dee et al., 2011) and observational data sets (e.g., E-OBS; Haylock et al., 2008; not shown).

To characterize the heatwave, we designed a novel detection algorithm, which focuses on the spatio-temporal evolution of extreme temperature patterns rather than on isolated local hot conditions (Perkins, 2015). This approach is particularly well suited to monitor large-scale heatwaves, which tend to affect different areas during their life cycle. To improve its performance, our algorithm uses T850 (as opposed to noisier T2m fields) and works as follows: (i) For each day, it identifies areas above 500,000 km^2 (oceans included) with daily mean T850 above the local daily 95th percentile of the 1981–2010 period, computed using a 31 day centered window. These spatial patterns also include noncontiguous areas if the distance between them is lower than 750 km. (ii) Two spatial patterns occurring in successive days are considered

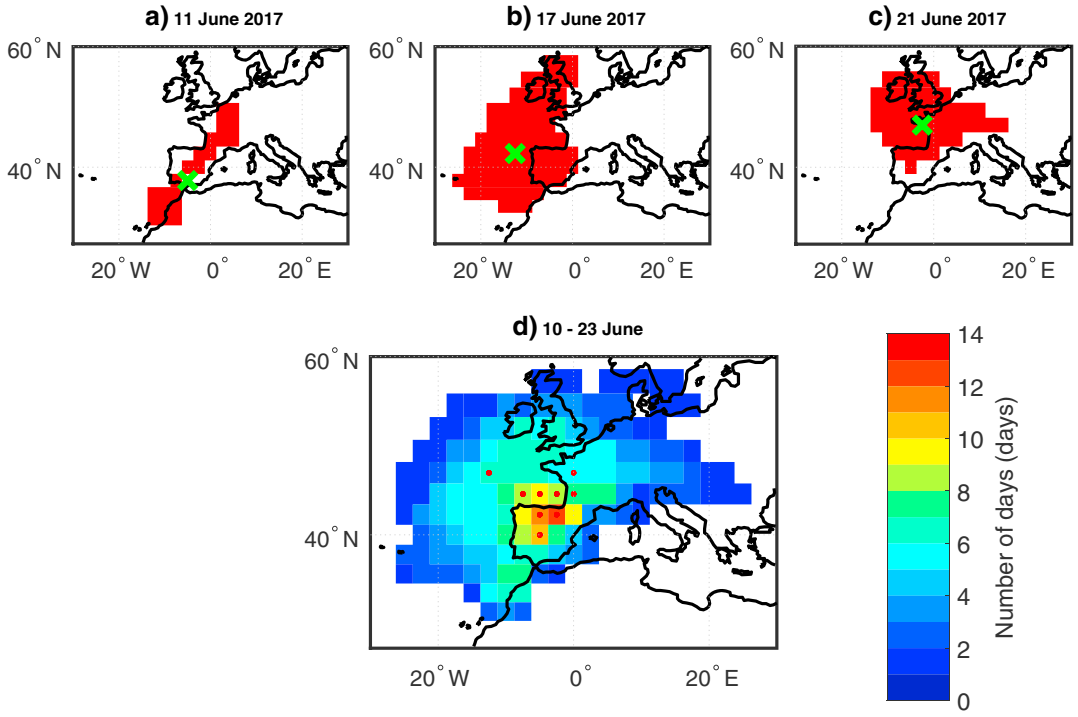

Figure 1. Spatio-temporal evolution of the June 2017 heatwave for selected days of (a) the onset, (b) the peak, and (c) the decaying phase. The regions under heatwave conditions are represented with red shading and the heatwave center with green crosses. (d) Total number of heatwave days (shading) for 10–23 June 2017, with red dots indicating regions where the heatwave persistence was record-breaking for June.

the same event if their areas overlap more than 50% or if there is any overlapping and the distance between their centers, defined as the area-weighted average of the standardized T850 anomalies, is less than 1000 km. (iii) If the event persists at least four consecutive days, it is considered a heatwave.

To describe the near-surface intensity of the heatwave event and quantify its exceptionality in the context of the reanalysis period, we identified the areas experiencing record-breaking T2m at different time-scales and characterized their temporal evolution, that is, following an approach similar to Barriopedro et al. (2011). To do so, we computed running means of T2m for windows ranging between 1 and 91 days and centered on each summer day of the 1948–2017 period (e.g., for the 7 day time-scale centered on 15 June 1950, the 12–18 June 1950 interval was averaged). For each grid-point, calendar day, and time-scale, the year with the largest value of the 1948–2016 period was retained as historical maximum. A record-breaking was identified if the corresponding 2017 value was higher than the historical maximum.

We characterized the atmospheric circulation during the heatwave event, exploring the connection with blocking and subtropical ridges. The blocking catalogue was computed using the Barriopedro et al. (2006) algorithm, which is based on the persistence (5 days) of large-scale (12.5°) reversals in the meridional Z500 gradient around typical latitudes of the extratropical jet stream. In addition, the algorithm from Sousa et al. (2017) was employed to diagnose the occurrence of subtropical ridges in the 30°W–30°E region. This data set provides ridge occurrence in four nonoverlapping longitudinal sectors of 15° width. For each sector, two conditions were imposed to detect a summer ridge in a given day: (i) at least 75% of the grid points within 35–55°N displayed Z500 values above the daily 80th percentile, computed from all 31 day centered windows of the analyzed period, and (ii) no more than 50% of the grid points within 55–75°N were above the same threshold. The latter criterion was included to avoid the detection of blocking patterns as subtropical ridges, thus ensuring that the same day is not catalogued as a blocking and a subtropical ridge simultaneously.

Flow analogues were used to characterize the interplay of the dynamics with the temperature anomaly during the heatwave episode (e.g., Yiou et al., 2014). Following Jézéquel et al. (2017), for each calendar day d of the event, we searched for the $N = 20$ days within the (d − 30, d + 30) interval of a reference period (excluding the target year) with the closest Z500 anomaly fields, as measured by the Euclidean distance over the 30–55°N,

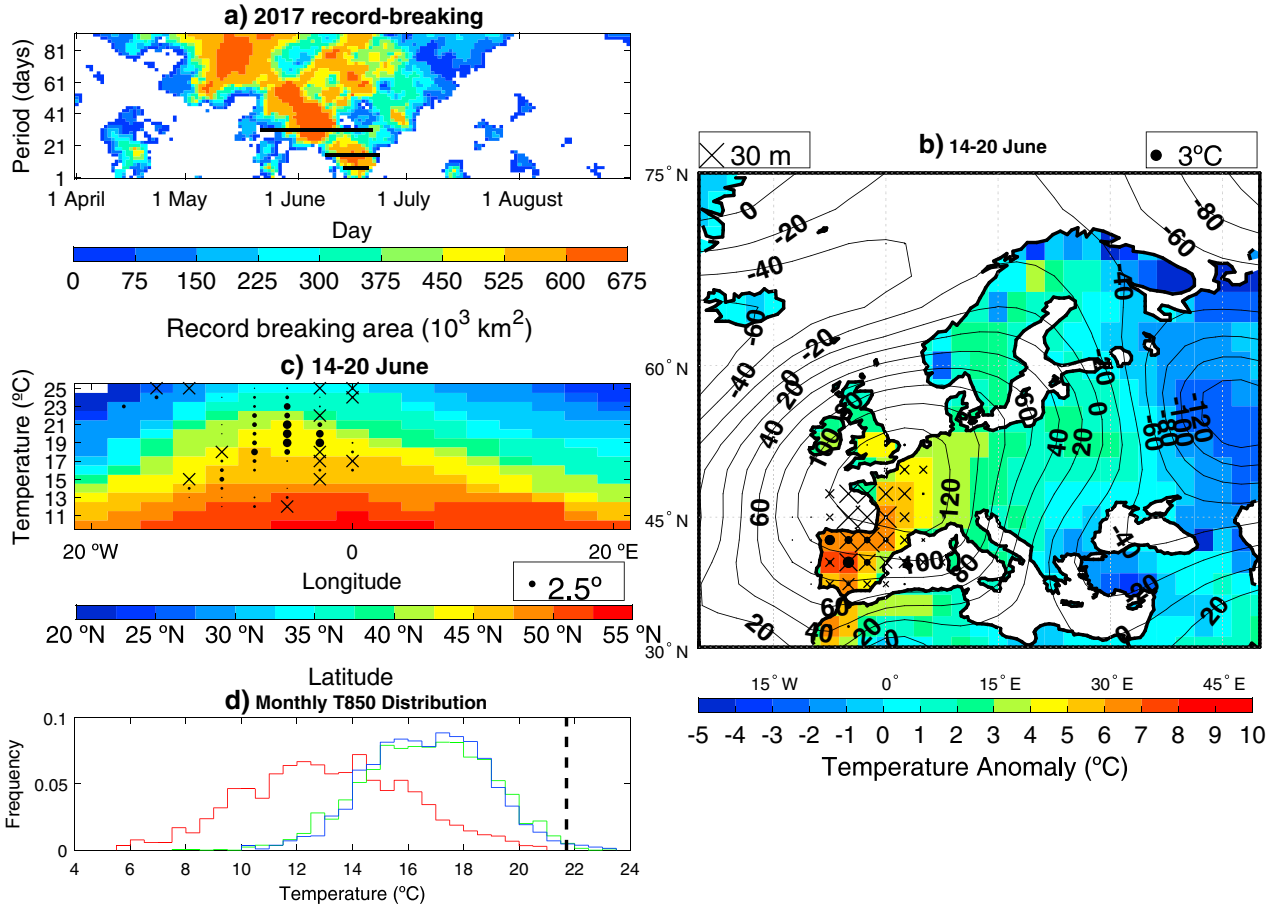

Figure 2. (a) Temporal evolution (*x* axis) of the spatial extent (in 10^3 km^2) of land areas over Iberia experiencing record-breaking T2m (with respect to the corresponding calendar day of the reanalysis period) on different time-scales (*y* axis). The black bars indicate the period of maximum extension for 7, 15, and 31 day time-scales. (b) Synoptic conditions for the 14–20 June 2017 period. The shading shows the T2m anomalies (in °C). The contours depict Z500 anomalies (in meter). Gridpoints with record-breaking T2m (Z500) are marked with black dots (crosses), with the size proportional to the exceedance over the previous record. (c) Longitudinal distribution (*x* axis) of the mean latitude (in °N, shading) of different 850 hPa isotherms (*y* axis) for the period 14–20 June 2017. The white color denotes missing values. The dots (crosses) highlight longitudes where the latitude of the corresponding isotherm was higher than (equal to) the previous record, with the size proportional to the record exceedance. (d) Frequency distribution of 7 day mean T850 (in °C) over Iberia in the reanalysis period for each summer month. The black vertical line shows the mean T850 for 14–20 June 2017.

10°W–15°E region. Different choices in the number of circulation analogues or spatial domain were tested, with similar results. We reconstructed the temperature anomalies during the heatwave period from the T2m anomalies of the circulation analogues, by picking one of the N analogues at random for each day. By repeating this process 100,000 times, we built the probability distribution of T2m anomaly driven by the observed atmospheric circulation. To assess whether the dynamics played a significant role, this analogue-based distribution was compared with that obtained randomly (Jézéquel et al., 2017). This process was performed by choosing random periods with the same length as the heatwave, thus accounting for persistence. Thus, we compared the reconstructed T2m anomalies from analogues of two reference periods (1948–1979 and 1980–2016, referred to as past and present, respectively).

3. Results

According to our detection algorithm, the June 2017 heatwave lasted 2 weeks, from 10 to 23 June. In the onset phase (Figure 1a), from 10 to 15 June, the event had an extension close to 1,000,000 km^2, affecting Iberia and southern France. The peak of the heatwave occurred between 16 and 18 June, when it embraced an area of 4,000,000 km^2, extending to the eastern Atlantic and the European Atlantic seaboard (Figure 1b). During the decaying phase (19–23 June), the event moved northeastward toward central Europe (Figure 1c).

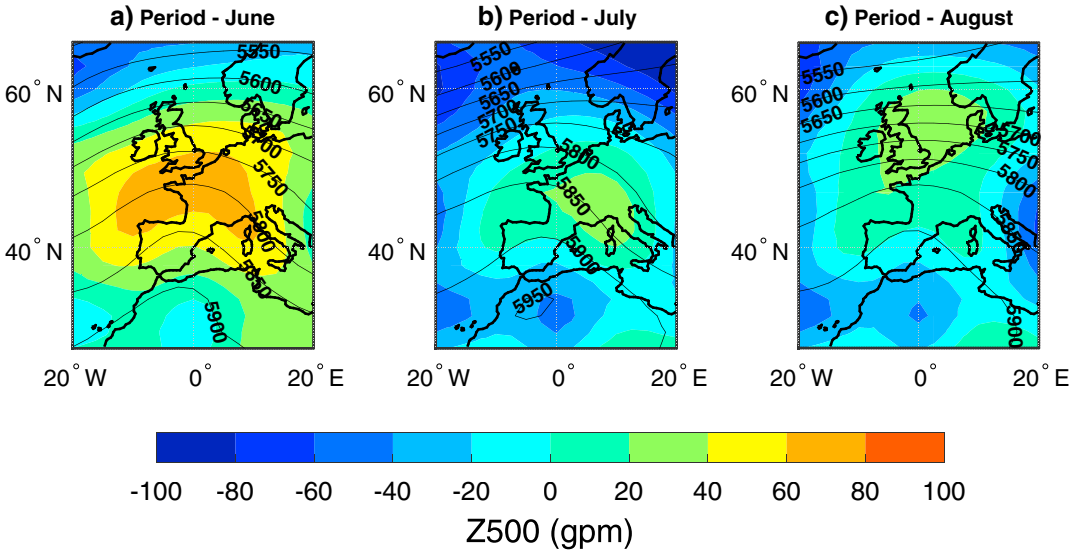

Figure 3. Spatial differences of the mean Z500 field (in gpm, shading) for the 15–21 June 2017 period and the composite (in gpm, contours) of all: (a) June, (b) July, and (c) August ridges over the 15°W–15°E sector.

As a whole, the total area under heatwave conditions was close to 8,000,000 km^2, including western and central Europe and the eastern Atlantic (Figure 1d). Iberia was the most affected area, with 12 heatwave days, being the longest June heatwave in this area for the reanalysis period. If all summer months are considered, this was the second longest heatwave in Iberia, following that of August 2003. Thus, the 2017 event fulfills the mega-heatwave criteria defined by Barriopedro et al. (2011). To compare this mega-heatwave with other summer episodes of the reanalysis period, we used the catalogue of Russo et al. (2015) for 1950–2015. Our algorithm successfully detected the 11 events included therein (see Table S1). Similar to the 2017 mega-heatwave, all considered events displayed extensions above 1,000,000 km^2, durations longer than 7 days, and local maximum intensities exceeding 2.5 standard deviations (see Table S2). However, the June 2017 event was the earliest one of the reanalysis period. To further compare these events, we also computed the HWMId of Russo et al. (2015), which aggregates the intensity and persistence of heatwave events, and the heatwave severity index (S) of Schoetter et al. (2015), which also accounts for areal extension. The 2017 event ranked the sixth (seventh) according to the S (HWMId) index (Table S2) and was the strongest one that affected Iberia (not shown).

To highlight the exceptionally of this event, Figure 2a shows the spatial extension of land areas over Iberia with record-breaking T2m throughout 1 April to 31 August 2017 at different time-scales. Between May and June, temperature records were broken over almost all Iberia at all the analyzed time-scales. At short time-scales (daily to fortnightly) the record-breaking values reached their maximum extension in mid-June, coinciding with the mega-heatwave period. Longer (monthly to seasonal) periods including the mega-heatwave interval also displayed record-breaking values over Iberia, but they were more widespread before than after the event. Consequently, generalized extreme hot conditions already started in spring and ended abruptly by late-June, despite the subsequent occurrence of short warm periods. Thus, the June event can be considered the extreme manifestation of a more persistent warm episode.

Figure 2b shows the atmospheric conditions for the 7 day peak (14–20 June; similar results were obtained for other time-scales). Iberia experienced 7 day mean T2m anomalies close to 10 °C, exceeding the previous records by up to 3 °C. Extreme conditions also extended to other regions (e.g., western France and southern British Islands), with temperature anomalies close to 5 °C and exceedances of ~1 °C above previous maxima. In the same period, the Z500 field was dominated by a conspicuous positive anomaly centered over France, with values up to 140 m, which exceeded historical maxima in Iberia and France by up to 30 m. This configuration, with positive Z500 anomalies extending from northern Africa to central Europe, suggests a subtropical intrusion of warm air over western Europe. To support this, we computed the mean latitudinal location of different 850 hPa isotherms for the 14–20 June period. Figure 2c reveals that there was a

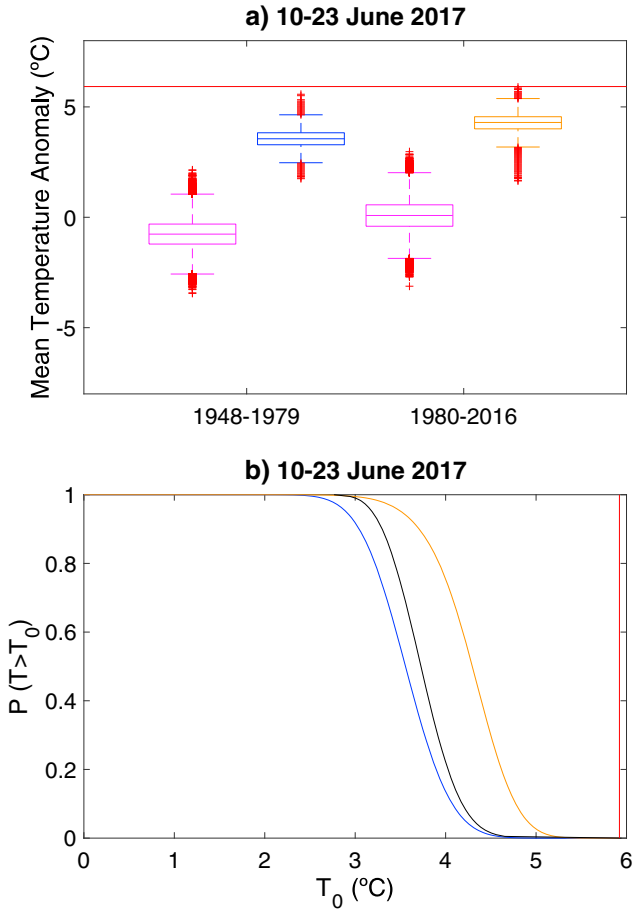

Figure 4. (a) Distributions of T2m anomalies (in °C) averaged over Iberia for 10–23 June 2017 as derived from random periods (purple boxplots) and Z500 flow analogues (blue and orange boxplots) of the past (1948–1979, two left boxplots) and present (1980–2016, two right boxplots) climate. (b) Flow-conditioned probability of exceeding a T2m threshold (T_0, *x* axis) over Iberia in the past (blue) and present (orange) climate. The black line represents the estimated contribution of dynamical changes, after adding the difference between the "thermodynamically adjusted" distributions to the past probability. In both panels the red line represents the observed T2m anomaly of the event over Iberia for 10–23 June 2017.

generalized northward displacement of the isotherms over the eastern Atlantic and western Europe (approximately 10°W–15°E), coinciding with regions of record-breaking T2m (Figure 2b). The 18–22 °C isotherms, which are typically located over northern Africa at this time of the year, shifted to Iberia, reaching its northernmost latitude for the reanalysis period, whereas those that are climatologically restricted to central Iberia (~12–13 °C) were pushed to the British Islands.

This temperature pattern, with the warm air mass extending from the south through a narrow longitudinal band, is in agreement with the possible influence of a subtropical ridge. However, previous European mega-heatwaves have also been associated to atmospheric blocking events. To better uncover the nature of the synoptic systems behind the Z500 anomaly, we used the ridge (Sousa et al., 2017) and blocking (Barriopedro et al., 2006) detection algorithms. No blocking events were detected during the summer of 2017 over the Euro-Atlantic sector (Figure S1), which represents an anomalously low frequency of episodes. Instead, there was a persistent ridge in the period 15–21 June over 15°W–15°E. As compared to all summer ridges affecting this sector in the 1950–2016 period, this event exhibited a record-breaking duration, equaling to that of 23–29 June 2005. The intensity of the ridge was also exceptional in a large area centered over western France, as revealed by the difference between the mean Z500 field for the 2017 ridge's lifecycle and the corresponding composite of all June ridges (Figure 3).

To further stress the role of circulation, Figure 4a shows the T2m anomaly distributions averaged over Iberia for the mega-heatwave period, as derived from the analogues of the past and present periods. We found similar results for different target periods (e.g., the entire June). The flow-conditioned T2m anomalies are significantly larger than their random distributions, indicating that the atmospheric conditions were favorable to the mega-heatwave, irrespective of the reference period. In fact, the dynamics played a dominant role, explaining ~73% of the observed T2m anomaly. The remaining T2m anomaly could partially be explained by amplifying factors not accounted for the circulation (e.g., SST anomalies or land-atmosphere feedbacks). The comparison between periods further reveals that T2m anomalies driven by circulation are higher in the present than would have been in the past (~60% of the observed T2m anomaly). This difference can be attributed to (i) dynamical changes, since the Euclidean distances of the flow analogues are significantly different between the two reference periods, with better analogues in the present than in the past (Figure S2a). The detection of dynamical changes is in agreement with a significant trend in the June frequency of subtropical ridges ($p < 0.01$); (ii) thermodynamical changes, as revealed by the difference of the T2m random distributions between periods, which is in good agreement with the mean warming of the region for June (~0.3 °C decade^{-1} for 1948–2017). If we assume that long-term changes in Z500 have been thermodynamically forced (e.g., Z500 rise by warming in lower levels) and remove Z500 and T2m trends, the so-called "thermodynamically adjusted" T2m distributions of the two reference periods become much closer (Figures S2b and S2c). This suggests a large thermodynamic contribution of climate change to Iberian temperatures, whatever the causes of the regional warming are.

Finally, we quantify how these changes have altered the odds of the mega-heatwave reaching a certain T2m anomaly, given the atmospheric circulation of the 2017. To do so, we computed the flow-conditioned probability of T2m anomalies above a given threshold by simply counting the fraction of replicates satisfying that condition for each reference period (e.g., Vautard et al., 2016). The results (Figure 3b) indicate that it is very likely that the observed circulation would have caused T2m anomalies above 3 °C in the past and present. However, the probability of experiencing T2m anomalies above 3.5 °C increases from 0.56 in the past to 0.95 in the present (almost a twofold increase). Under the same circulation, the chances of exceeding 4 °C

have increased by a factor of 5. Dynamical changes, herein defined as the difference between the "thermodynamically adjusted" probabilities of both periods, have contributed to moderate T2m anomalies (up to ~3.5 °C), while thermodynamical trends are largely responsible for the risk ratio of more extreme thresholds (Figure 4b).

4. Concluding Remarks

The June 2017 mega-heatwave lasted two weeks, affected a wide area of up to 8,000,000 km^2 from the east Atlantic to western and central Europe, and displayed an outstanding intensity, being the sixth (seventh) strongest European summer event of the reanalysis period according to the S (HWMId) index. The main threatened area was Iberia, where this event was the strongest summer heatwave and the most persistent one of all June heatwaves in the reanalysis period, causing the warmest temperatures from daily to seasonal time-scales of the corresponding calendar dates. The Portuguese forest fires were the most relevant impact.

The advanced timing is perhaps the most prominent feature of this event. In fact, it was the earliest mega-heatwave in Europe since at least the midtwentieth century, being preceded by an extremely hot and dry late spring (García-Herrera et al., 2018). The atmospheric circulation was largely responsible for the observed temperature anomalies, and it was characterized by a long-lasting subtropical ridge, whose signatures were closer to those of July and August ridges (Figures 4b and 4c). Thus, it could be viewed as a high-summer ridge occurring earlier than expected. The high-summer character of this June event is also seen in Figure 2d, which shows that the 14–20 June week not only was the warmest one of all Junes in Iberia but also fell beyond the 99th percentiles of the weekly T850 distributions for July and August.

Summing up, the June 2017 mega-heatwave could be an actual manifestation of summers that are becoming longer and with an earlier onset (Peña-Ortiz et al., 2015), in agreement with future projections of global warming scenarios (Cassou & Cattiaux, 2016). Accordingly, we find that the observed circulation caused higher temperatures in Iberia than those expected from past analogues due to recent changes in dynamics and thermodynamics. The latter were more important in explaining the exceptional temperatures, and very likely made this two-week event at least ~0.7 °C warmer on average.

Acknowledgments
We acknowledge the Earth System Research Laboratory (ESRL) Physical Sciences Division, Boulder, Colorado, USA for providing the NCEP/NCAR reanalysis data (www.esrl.noaa.gov/psd). This work was supported by the Ministerio de Economía y Competitividad through the PALEOSTRAT (CGL2015-69699-R) and ISIPEDIA (ERA4CS) (PCIN-2017-046) projects. Ricardo M. Trigo and Pedro M. Sousa are supported by project IMDROFLOOD: Improving Drought and Flood Early Warning, Forecast and Mitigation using real-time hydroclimatic indicators, JPND-WaterJPI/0004/2014, financed by FCT/MCTES (PIDDAC). A. Sánchez-Benítez was funded by grant FPU15/03958 from the Ministerio de Educación, Cultura y Deporte (MECD).

References

Bador, M., Terray, L., Boe, J., Somot, S., Alias, A., Gibelin, A., & Dubuisson, B. (2017). Future summer mega-heatwave and record-breaking temperatures in a warmer France climate. *Environmental Research Letters*, *12*(7), 074025. https://doi.org/10.1088/1748-9326/aa751c

Barriopedro, D., Fischer, E., Luterbacher, L., Trigo, R., & García-Herrera, R. (2011). The hot summer of 2010: Redrawing the temperature record map of Europe. *Science*, *332*(6026), 220–224. https://doi.org/10.1126/science.1201224

Barriopedro, D., García-Herrera, R., Lupo, A., & Hernández, E. (2006). A climatology of northern hemisphere blocking. *Journal of Climate*, *19*(6), 1042–1063. https://doi.org/10.1175/JCLI3678.1

Carmona, R., Linares, C., Ortíz, C., Mirón, I., Luna, M., & Díaz, J. (2017). Spatial variability in threshold temperatures of heat wave mortality: Impact assessment on prevention plans. *International Journal of Environmental Health Research*, 1–13. https://doi.org/10.1080/09603123.2017.1379056

Cassou, C., & Cattiaux, J. (2016). Disruption of the European climate seasonal clock in a warming world. *Nature Climate Change*, *6*(6), 589–594. https://doi.org/10.1038/nclimate2969

Climate Central (2017). European Heat, June 2017. Retrieved from https://wwa.climatecentral.org/analyses/europe-heat-june-2017/

Dee, D., Uppala, S., Simmons, A., Berrisford, P., Poli, P., Kobayashi, S., … Vitart, F. (2011). The ERA-INTERIM reanalysis: Configuration and performance of the data assimilation system. *Quarterly Journal of the Royal Meteorological Society*, *137*(656), 553–597. https://doi.org/10.1002/qj.828

Della-Marta, P., Luterbacher, J., von Weissenfluh, H., Xoplaki, E., Brunet, M., & Wanner, H. (2007). Summer heat waves over western Europe 1880–2003, their relationship to large-scale forcings and predictability. *Climate Dynamics*, *29*(2-3), 251–275. https://doi.org/10.1007/s00382-007-0233-1

Dole, R., Hoerling, M., Perlwitz, J., Eischeid, J., Pegion, P., Zhang, T., … Murray, D. (2011). Was there a basis for anticipating the 2010 Russian heat wave? *Geophysical Research Letters*, *38*, L06702. https://doi.org/10.1029/2010GL046582

Duchez, A., Frajka-Williams, E., Josey, S., Evans, D., Grist, J., Marsh, R., … Hirschi, J. (2016). Drivers of exceptionally cold North Atlantic Ocean temperatures and their link to the 2015 European heat wave. *Environmental Research Letters*, *11*(7), 074004. https://doi.org/10.1088/1748-9326/11/7/074004

Fischer, E. (2014). Climate science: Autopsy of two mega-heatwaves. *Nature Geoscience*, *7*(5), 332–333. https://doi.org/10.1038/ngeo2148

Fischer, E., Seneviratne, S., Lüthi, D., & Schär, C. (2007). The contribution of land-atmosphere coupling to recent European summer heat-waves. *Geophysical Research Letters*, *34*, L06707. https://doi.org/10.1029/2006GL029068

Fouillet, A., Rey, G., Laurent, F., Pavillon, G., Bellec, S., Guihenneuc-Jouyaux, C., … Hémon, D. (2006). Excess mortality related to the August 2003 heat wave in France. *International Archives of Occupational and Environmental Health*, *80*(1), 16–24. https://doi.org/10.1007/s00420-006-0089-4

García-Herrera, R., Díaz, J., Trigo, R., Luterbacher, J., & Fischer, E. (2010). A review of the European summer heat wave of 2003. *Critical Reviews in Environmental Science and Technology*, *40*(4), 267–306. https://doi.org/10.1080/10643380802238137

García-Herrera, R., Garrido-Pérez J., Barriopedro, D., Ordoñez C, Vicente-Serrano S., Nieto R., … Yiou P. (2018). *The severe drought of 2016–2017 in Western Europe*. Paper presented at European Geosciences Union General Assembly 2018, Vienna, Austria.

Gouveia, C., Bistinas, I., Liberato, M., Bastos, A., Koutsias, N., & Trigo, R. (2016). The outstanding synergy between drougtht, heatwaves and fuel on the 2007 Southern Greece exceptional fire season. *Agricultural and Forest Meteorology*, *218-219*, 135–145. https://doi.org/10.1016/j.agrformet.2015.11.023

Haines, A., Kovats, R., Campbell-Lendrum, D., & Corvalan, C. (2006). Climate change and human health: Impacts, vulnerability and public health. *Public Health*, *120*(7), 585–596. https://doi.org/10.1016/j.puhe.2006.01.002

Haylock, M., Hofstra, N., Klein Tank, A., Klok, E., Jones, P., & New, M. (2008). A European daily high-resolution gridded data set of surface temperature and precipitation. *Journal of Geophysical Research*, *113*, D20119. https://doi.org/10.1029/2008JD010201

Hodzic, A., Madronich, S., Bohn, B., Massie, S., Menut, L., & Wiedinmyer, C. (2007). Wildfire particulate matter in Europe during summer 2003: Meso-scale modelling of smoke emissions, transport and radiative effects. *Atmospheric Chemistry and Physics*, *7*, 4043–4064. https://doi.org/10.5194/acp-7-4043-2007

Jézéquel, A., Yiou, P., & Radanovics, S. (2017). Role of circulation in European heatwaves using flow analogues. *Climate Dynamics*, 1–15. https://doi.org/10.1007/s00382-017-3667-0

Kalnay, E., Kanamitsu, M., Kistler, R., Collins, W., Deaven, D., Gandin, L., … Joseph, D. (1996). The NCEP/NCAR 40-Year Reanalysis Project. *Bulletin of the American Meteorological Society*, *77*(3), 437–471. https://doi.org/10.1175/1520-0477(1996)077%3C0437:TNYRP%3E2.0.CO;2

Kalvelage, K., Passe, U., Rabideau, S., & Takle, E. (2014). Changing climate: The effects on energy demand and human comfort. *Energy and Buildings*, *76*, 373–380. https://doi.org/10.1016/j.enbuild.2014.03.009

Kirch, W., Menne, B., & Bertollini, R. (Eds.) (2005). *Extreme Weather Events and Public Health Responses*. Berlin: Springer-Verlag. https://doi.org/10.1007/3-540-28862-7

Konovalov, I., Beekmann, M., Kuznetsova, I., Yurova, A., & Zyvagintsev, A. (2011). Atmospheric impacts of the 2010 Russian wildfires: Integrating modelling and measurements of an extreme air pollution episode in the Moscow region. *Atmospheric Chemistry and Physics*, *11*(19), 10,031–10,056. https://doi.org/10.5194/acp-11-10031-2011

Kovats, R., & Hajat, S. (2008). Heat stress and public health: A critical review. *Annual Review of Public Health*, *29*(1), 41–55. https://doi.org/10.1146/annurev.publhealth.29.020907.090843

Lesk, C., Rowhani, P., & Ramankutty, N. (2016). Influence of extreme weather disasters on global crop production. *Nature*, *529*(7584), 84–87. https://doi.org/10.1038/nature16467

Lowe, D., Ebi, K., & Forsberg, B. (2011). Heatwave early warning systems and adaptation advice to reduce human health consequences of heatwaves. *International Journal of Environmental Research and Public Health*, *8*(12), 4623–4648. https://doi.org/10.3390/ijerph8124623

Meehl, G., & Tebaldi, C. (2004). More intense, more frequent, and longer lasting heat waves in the 21st century. *Science*, *305*(5686), 994–997. https://doi.org/10.1126/science.1098704

Meteofrance (2017). June 2017 monthly climatological report. Retrieved from http://www.meteofrance.fr/actualites/51243610-juin-2017-2e-plus-chaud-depuis-1900

Meteosuisse (2017). June 2017 monthly climatological report. Retrieved from http://www.meteoschweiz.admin.ch/home/aktuell/meteoschweiz-blog/meteoschweiz-blog.subpage.html/de/data/blogs/2017/6/aussergewoehnlich-heisser-juni.html#comments

Miralles, D., Teuling, A., van Heerwaarden, C., & Vilá-Guerau, J. (2014). Mega-heatwave temperatures due to combined soil desiccation and atmospheric heat accumulation. *Nature Geoscience*, *7*(5), 345–349. https://doi.org/10.1038/ngeo2141

Peña-Ortíz, C., Barriopedro, D., & García-Herrera, R. (2015). Multidecadal variability of the summer length in Europe. *Journal of Climate*, *28*(13), 5375–5388. https://doi.org/10.1175/JCLI-D-14-00429.1

Perkins, S. (2015). A review on the scientific understanding of heatwaves—Their measurement, driving mechanisms, and changes at the global scale. *Atmospheric Research*, *164-165*, 242–267. https://doi.org/10.1016/j.atmosres.2015.05.014

Pfahl, S. (2014). Characterising the relationship between weather extremes in Europe and synoptic circulation features. *Natural Hazards and Earth System Sciences*, *14*(6), 1461–1475. https://doi.org/10.5194/nhess-14-1461-2014

Royal Netherlands Meteorological Institute (KNMI) (2017). June 2017 monthly climatological report. Retrieved from https://www.knmi.nl/nederland-nu/klimatologie/maand-en-seizoensoverzichten/2017/juni

Russo, S., Sillmann, J., & Fischer, E. (2015). Top ten European heatwaves since 1950 and their occurrence in the coming decades. *Environmental Research Letters*, *10*, 054016. https://doi.org/10.1088/1748-9326/10/12/124003

Schoetter, R., Cattiaux, J., & Douville, H. (2015). Changes of western European heat wave characteristics projected by the CMIP5 ensemble. *Climate Dynamics*, *45*(5-6), 1601–1616. https://doi.org/10.1007/s00382-014-2434-8

Seneviratne, S., Corti, T., Davin, E., Hirschi, M., Jaeger, E., Lehner, I., … Teuling, A. (2010). Investigating soil moisture-climate interactions in a changing climate: A review. *Earth-Science Reviews*, *99*, 125–161. https://doi.org/10.1016/j.earscirev2010.02.004

Sousa, P., Trigo, R., Barriopedro, D., Soares, P., & Santos, J. (2017). European temperatures responses to blocking and ridge regional patterns. *Climate Dynamics*, 1–21. https://doi.org/10.1007/s00382-017-3620-2

Spanish Meteorological Agency (AEMET) (2017). June 2017 monthly climatological report. Retrieved from http://www.aemet.es/documentos/es/serviciosclimaticos/vigilancia_clima/resumenes_climat/mensuales/2017/res_mens_clim_2017_06.pdf

Trigo, R., García-Herrera, R., Díaz, J., Trigo, I., & Valente, M. (2005). How exceptional was the early August 2003 heatwave in France? *Geophysical Research Letters*, *32*, L10701. https://doi.org/10.1029/2005GL022410

Vautard, R., Honoré, C., Beekmann, M., & Rouil, L. (2005). Simulation of ozone during August 2003 heat wave and emission control scenarios. *Atmospheric Environment*, *39*(16), 2957–2967. https://doi.org/10.1016/j.atmosenv.2005.01.039

Vautard, R., Yiou, P., Otto, F., Stott, P., Christidis, N., van Oldenborgh, G. J., & Schaller, N. (2016). Attribution of human-induced dynamical and thermodynamical contributions in extreme weather events. *Environmental Research Letters*, *11*(11), 114009. https://doi.org/10.1088/1748-9326/11/11/114009

Yiou, P., Boichu, M., Vautard, R., Vrac, M., Jourdain, S., Garnier, E., … Menut, L. (2014). Ensemble meteorological reconstruction using circulation analogues of 1781-1785. *Climate of the Past*, *10*(2), 797–809. https://doi.org/10.5194/cp-10-797-2014